Effects of Spanwise Blowing and Reverse Thrust on Fighter Low-Speed Aerodynamics

J.W. Paulson Jr.,* D.W. Banks,* and P.F. Quinto*
NASA Langley Research Center, Hampton, Virginia

A brief review of takeoff and landing requirements for the next generation of fighter aircraft indicates that improvement in lift performance and thrust reversing capability will be needed if short takeoff and landing (STOL) operations are to be feasible. A recent joint NASA/Grumman Aerospace Corporation/U.S. Air Force Wright Aeronautical Laboratory wind tunnel investigation was conducted to examine the effects of spanwise blowing on the trailing-edge flap system. This application contrasts with the more familiar method of spanwise blowing near the wing leading edge. Another joint program among NASA/McDonnell Aircraft Company/U.S. Air Force Wright Aeronautical Laboratory investigated the effects of reverse thrust on the low-speed aerodynamics of an F-15 configuration. The F-15 model was fitted with a rotating vane thrust reverser concept which could simulate both in-flight reversing for approach and landing or full reversing for ground roll reduction. The significant results of these two joint programs are reported in this paper.

Nomenclature

a = acceleration, m/s^2 (ft/s^2)
b = wing span, m (ft)
c = wing mean aerodynamic chord, m (ft)
C_D = drag coefficient = drag/qS
$C_{D,0}$ = minimum drag coefficient
C_L = lift coefficient = lift/qS
$C_{L,0}$ = lift coefficient at $\alpha = 0$ deg
C_{L_α} = lift-curve slope = $\partial C_L/\partial\alpha$
C_m = pitching-moment coefficient = pitching moment/qSc
$C_{m,0}$ = pitching-moment coefficient at zero lift
C_{m_α} = pitching-moment stability derivative = $\partial C_m/\partial\alpha$
$C_{m_{\delta_{HT}}}$ = horizontal tail effectiveness = $\partial C_m/\partial\delta_{HT}$
C_n = yawing-moment coefficient = yawing moment/qSb
C_{n_β} = directional stability derivative = $\partial C_n/\partial\beta$
$C_{n_{\delta_R}}$ = rudder effectiveness = $\partial C_n/\partial\delta_R$
C_T = static thrust coefficient = static thrust/qS
C_μ = ideal thrust coefficient = ideal thrust/qS
$\Delta C_{L,\Gamma}$ = thrust-induced increment in lift coefficient = $C_{L_{C_{T\geq 0}}} - C_T\sin(\alpha+\theta_j) - C_{L_{C_{T=0}}}$
g = gravitational constant = 9.807 m/s^2 (32.174 ft/s^2)
NPR = nozzle pressure ratio = $p_{t,j}/p_\infty$
$p_{t,j}$ = nozzle total pressure, kPa (lb/ft^2)
p_∞ = freestream static pressure, kPa (lb/ft^2)
q = freestream dynamic pressure, kPa (lb/ft^2)
W/S = wing loading, N/m^2 (lb/ft^2)
α = angle of attack, deg
β = yaw angle, deg
γ = flight-path angle, deg
δ = deflection angle, deg
θ_j = jet deflection angle, deg

Subscripts

HT = horizontal tail
R = rudder
REV = reverser

Notation

50 deg/50 deg = symmetrical nozzle deflection, 50 deg upper and 50 deg lower
70 deg/70 deg = symmetrical nozzle deflection, 70 deg upper and 70 deg lower
90 deg/50 deg = asymmetrical nozzle deflection, 90 deg upper and 50 deg lower
130 deg/130 deg = symmetrical nozzle deflection, 130 deg upper and 130 deg lower

Introduction

WITH the recent interest in STOL performance for fighter aircraft, the NASA Langley Research Center has undertaken a program to help define and develop the technologies required for low-speed flight of advanced fighter/attack configurations with emphasis on STOL operations. This effort includes research on advanced high-lift systems using mechanical flaps; thrust vectoring; thrust-induced effects; methods of obtaining longitudinal trim when using thrust vectoring; and reverse thrust for decreased ground rolls.

The need for these technologies is shown in Figs. 1-3. Ground roll distances for both takeoff and landing (Fig. 1) indicate that present day fighter aircraft can become airborne in relatively short distances [300-375 m (985-1230 ft)], but they have little or no short field capability for landing as indicated by ground roll distances of about 800 m (2625 ft). One potential solution to balance the field lengths (i.e., have equal takeoff and landing ground rolls) is to incorporate an efficient thrust reverser into the airplane design (Fig. 2). In Fig. 2, it can be seen that if maximum wheel braking and reverse thrust (50% of military power) can be employed at wheel touchdown, then landing ground rolls on the order of from 300 to 395 m (985-1230 ft) can be obtained at approach lift coefficients of about 1.0. It should be noted that this level of lift will not be a significant increase from present day approach lift coefficients. However, if the ground roll requirement becomes less than 305 m (1000 ft), then the

Presented as Paper 81-2612 at the AIAA/NASA Ames V/STOL Conference, Palo Alto, Calif., Dec. 7-9, 1981; submitted Dec. 16, 1981; revision received April 23, 1982. This paper is declared a work of the U.S. Government and therefore is in the public domain.

*Aerospace Engineer, Subsonic Aerodynamics Branch. Member AIAA.

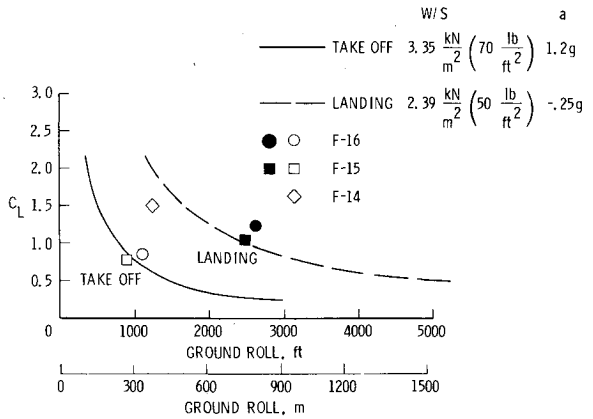

Fig. 1 Fighter takeoff and landing ground rolls.

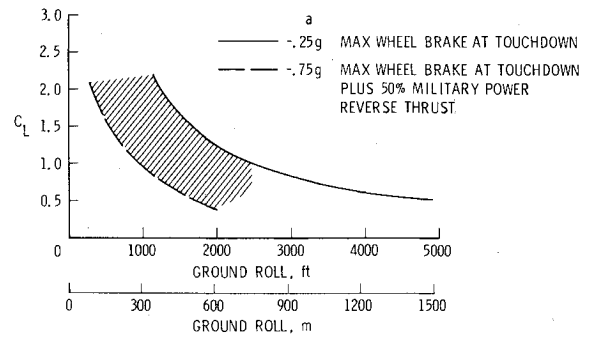

Fig. 2 Effect of lift coefficient and reverse thrust on landing ground roll.

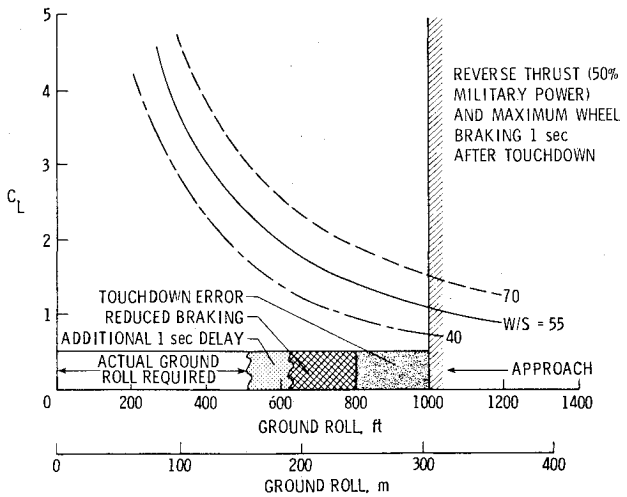

Fig. 3 Approach lift coefficient vs landing ground roll for fighter aircraft.

approach lift coefficient must increase dramatically. In Fig. 3, a slightly conservative approach (i.e., wheel braking and reverse thrust 1 s after wheel touchdown) still yields a landing ground roll of 305 m (1000 ft) at only modest increases in present approach lift coefficients. But, there can be a vast difference in the performance required of an aircraft if it is allowed only 305 m (1000 ft) of usable runway rather than ground roll. If touchdown dispersion, reduced braking (i.e., wet or icy runway), and 1-s piloting delay are also considered, then the aircraft must be capable of operations from a 150-m (500-ft) ground roll which require approach lift coefficients on the order of 2.5. This level of lift coefficient can be obtained on conventional fighter-type configurations only through the use of some form of powered lift.

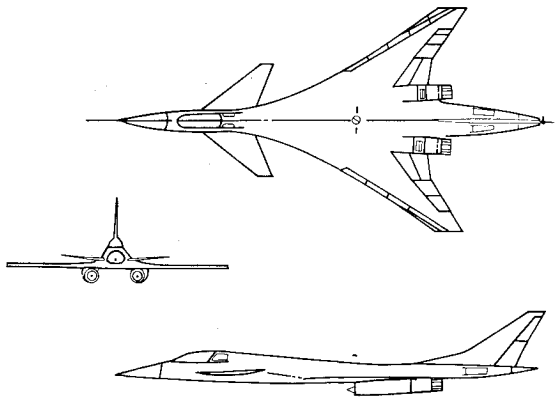

Fig. 4 Grumman advanced fighter configuration.

Discussion

NASA Langley has conducted several wind tunnel investigations on three separate advanced fighter configurations in an effort to define the aerodynamic effects of various forms of vectored thrust. These results have been published in several references[1-10] and their discussion is not included in this paper. However, with this background in power-induced effects, NASA Langley is currently involved in several joint programs to investigate other means of generating high lift, obtaining longitudinal trim, and developing a knowledge of reverse thrust effects. The remainder of this paper will discuss two recent wind tunnel studies: 1) a joint NASA/Grumman Aerospace Corporation/U.S. Air Force Wright Aeronautical Laboratory (AFWAL) investigation of the effects of spanwise blowing on a trailing-edge flap system, and 2) a joint NASA/McDonnell Aircraft Company (MACAIR)/AFWAL investigation of the effect of reverse thrust on the low-speed aerodynamics of an F-15 configuration.

Effects of Spanwise Blowing on the Trailing-Edge Flap

Grumman is under contract with AFWAL to develop advanced exhaust nozzles for survivable STOL aircraft. This effort is being supported by NASA through wind tunnel testing and analysis. The baseline Grumman configuration is shown in Fig. 4, and it was proposed that a method of generating increased lift might be to blow exhaust air spanwise along the flap either above or below the wing. Since there was remarkable similarity between the planforms of the Grumman configuration and the NASA close-coupled wing-canard configuration,[1-5] it was decided that the NASA model could be modified to incorporate the Grumman nacelle, primary nozzles, spanwise blowing nozzles, and trailing-edge flap systems. The assembled model is shown in Fig. 5, and the new hardware along with the modified NASA wing is shown in Fig. 6. A photograph of the under-the-wing spanwise blowing nozzle (cascade), shown in Fig. 7, indicates the location of the cascade below and forward of the trailing-edge flap. The cascades were intended to divert a large (20-60%) portion of exhaust mass flow in the spanwise direction at three vector angles (i.e., 0 deg, perpendicular to nacelle center line; 30 deg, parallel to flap hinge line; and −30 deg, blowing forward). It was anticipated that the spanwise cascade exhaust flow would mix with the freestream, turn downstream, and be turned by the trailing-edge flap in a manner not unlike an externally blown flap. A photograph of the above-the-wing spanwise blowing nozzle (port), shown in Fig. 8, indicates the port location above and just aft of the upper surface of the flap. The ports were intended to divert a small (5-10%) portion of the exhaust mass flow in the spanwise direction at three vector angles (i.e., 30 deg parallel to flap hinge line and 45 and 60 deg or 15 and 30 deg, aft of the hinge line). The spanwise port exhaust flow would set up a vortex on the upper surface of the flap which would help maintain attached flow on the highly deflected flap.

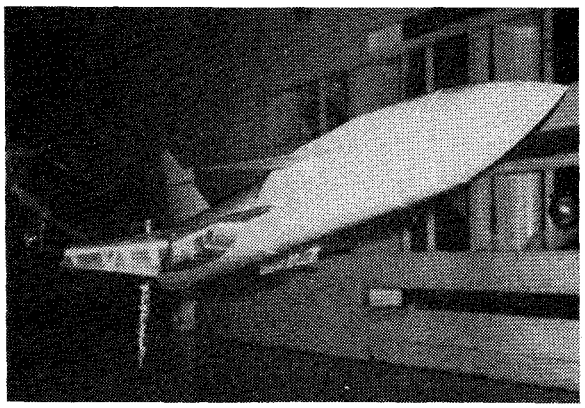

Fig. 5 Modified NASA wing-canard fighter model installed in the NASA Langley 4- by 7-Meter Tunnel.

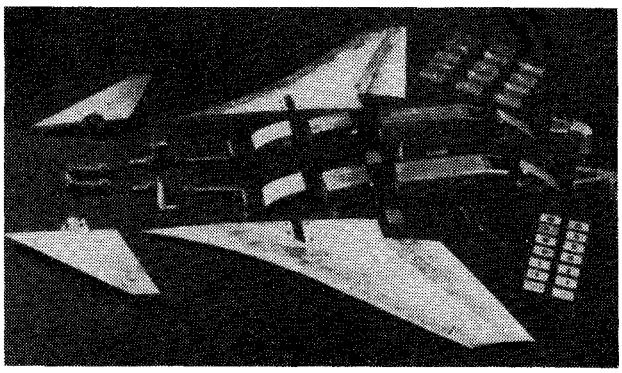

Fig. 6 New model parts for NASA wing-canard fighter model.

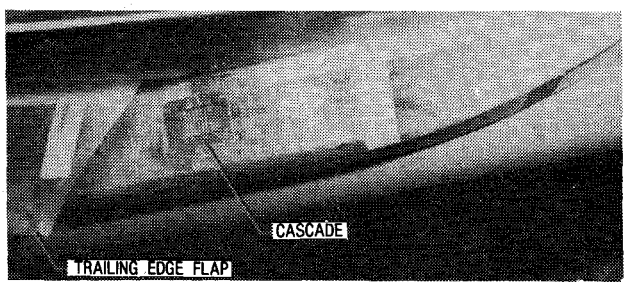

Fig. 7 Below wing cascade on nacelle of modified NASA wing-canard fighter model.

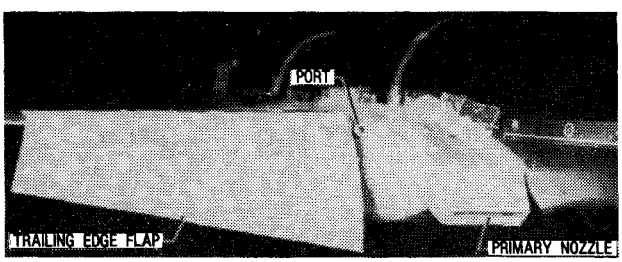

Fig. 8 Above wing port on modified NASA wing-canard fighter model.

During the test all cascades and ports were tested in a screening process to determine the most effective configurations at nominal approach angles of attack (i.e., 12, 14, and 16 deg), and these configurations were then investigated over more complete angle-of-attack ranges. This screening process is omitted for this paper and a discussion of two cascades and one port will follow. The definition for a most effective configuration was the largest induced lift for a given mass flow; that is, if two cascades generated the same $\Delta C_{L,\Gamma}$,

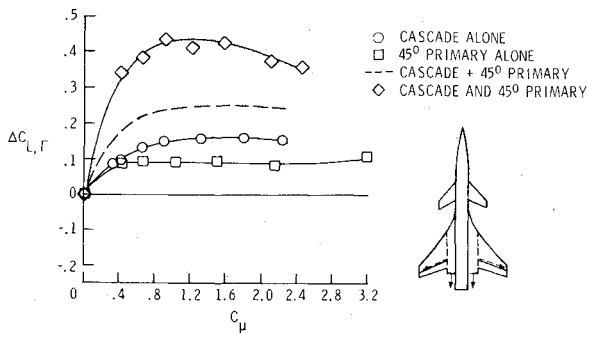

Fig. 9 Induced lift for cascade blowing parallel to flap hinge line.

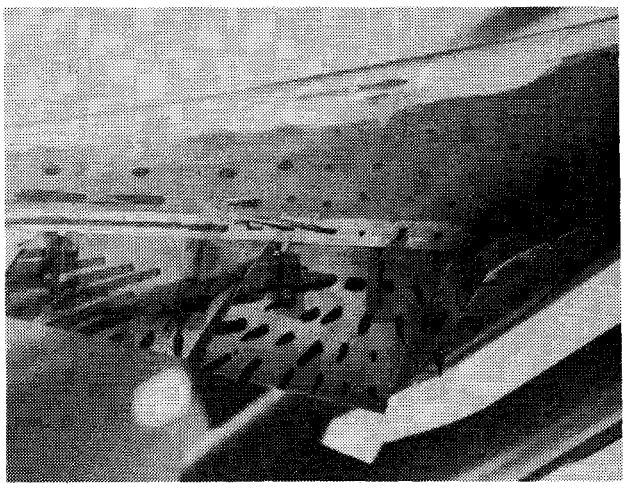

Fig. 10 Oil flow with cascade blowing parallel to flap hinge line.

then the cascade with the smallest mass flow would be investigated over a complete angle-of-attack range. A similar rationale was used to determine the most effective port.

An example of the $\Delta C_{L,\Gamma}$ for a cascade is shown in Fig. 9. Data are shown for the primary nozzle alone, cascade alone, and primary nozzle plus cascade. This cascade was intended to divert 60% of exhaust mass flow parallel to the flap hinge line. It can be seen that the primary nozzle at $\delta_N = 45$ deg gives a constant $\Delta C_{L,\Gamma} \simeq 0.1$ at all $C_\mu \geq 0.4$. The induced lift from the cascade alone is on the order of 0.15 and is constant above $C_\mu \simeq 0.8$. The induced lift for the combination of 45-deg primary nozzle deflection and 30-deg cascade has a maximum of about 0.43 which is considerably greater than the numerical addition of the primary plus the cascade, indicating a substantial beneficial interference. The mechanism of this interference is being investigated further, but, at present, is unknown. At the maximum $\Delta C_{L,\Gamma} \simeq 0.43$, the total lift coefficient for the configuration was $C_L = 2.18$. Therefore the thrust-induced lift was about 20% of the total lift. Compared to the induced-lift increments seen in previous configurations,[4,5] this rather substantial amount of induced lift indicates that the spanwise blowing is distributing the flow over a large portion of the wing trailing edge. This conclusion was confirmed in the oil flow studies done during the test, as shown in Fig. 10. The trace of the spanwise flow is clearly shown out to the wing tip. The inboard flap, however, does not appear to be affected as the spanwise flow penetrates outboard before expanding and turning to impinge on the outboard flap. Since a portion of the trailing edge was not affected by the spanwise flow, it would appear that these rather substantial induced increments will be increased when the spanwise jet is distributed over the entire trailing-edge flap.

The induced lift for an alternate cascade configuration which also diverted 60% of exhaust flow, but which exited

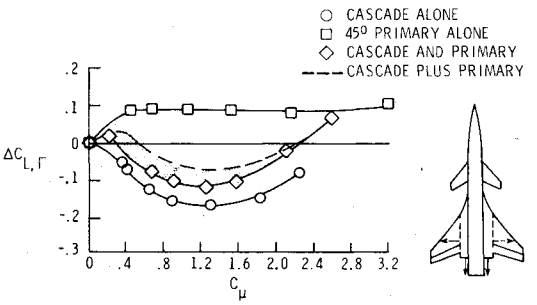

Fig. 11 Induced lift with cascade blowing perpendicular to body centerline.

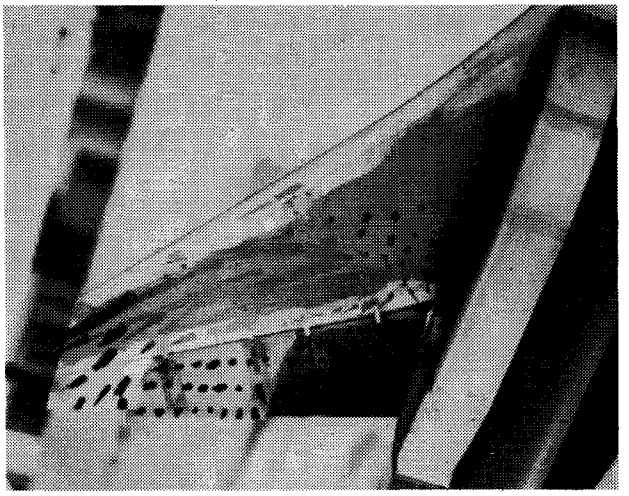

Fig. 12 Oil flow with cascade blowing perpendicular to body centerline.

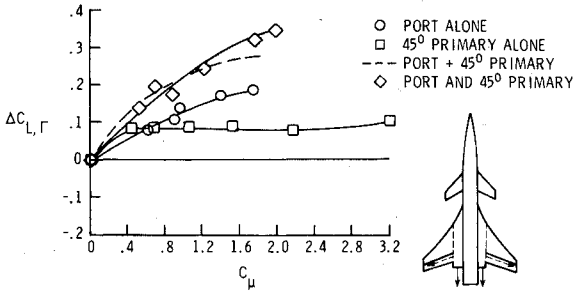

Fig. 13 Induced lift for port blowing parallel to flap hinge line.

normal to the nacelle rather than parallel to the flap hinge line, is shown in Fig. 11. The oil flow for this condition is shown in Fig. 12. Induced lift losses were experienced as the spanwise jet blew off the wing tip and never turned to impinge on the trailing-edge flap.

The induced lift increment for a port is shown in Fig. 13 and the oil flow in Fig. 14. This port diverted 10% of exhaust mass flow parallel to the flap hinge line. The primary nozzle with δ_N of 45 deg produced a constant $\Delta C_{L,\Gamma} \simeq 0.1$. The port alone produced $\Delta C_{L,\Gamma}$ up to 0.2, and the combined port and primary nozzle are only slightly greater than the numerical sum of the primary plus port, indicating minimal interference between the flows on the upper and lower surfaces. Again, the trace of the spanwise jet is clearly seen in the flow photograph. It passes over the inboard and outboard flap and beneath the end of the undeflected wing tip.

As mentioned earlier, the cascade parallel to the flap hinge line produced about 20% of the total configuration lift through induced effects. To assess the usefulness of this increment, the total configuration longitudinal aerodynamics

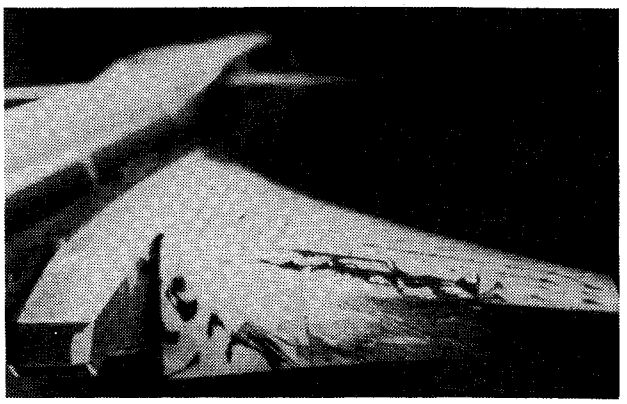

Fig. 14 Oil flow with port blowing parallel to flap hinge line.

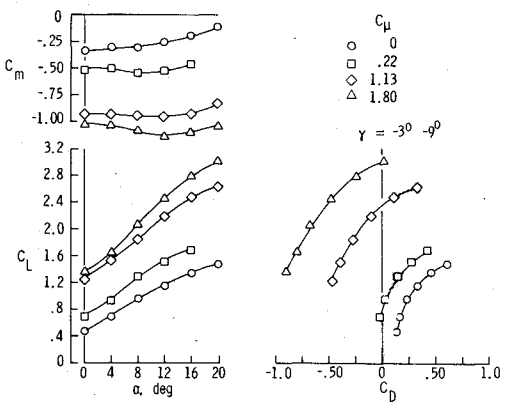

Fig. 15 Longitudinal aerodynamics with cascade blowing parallel to flap hinge line, primary nozzles deflected 45 deg and flaps deflected 45 deg/45 deg.

are presented in Fig. 15. It is seen here that although C_L and C_D are appropriate for a landing condition (i.e., $C_L \simeq 2.4$ at $\alpha = 16$ deg, with $C_\mu \simeq 1.13$ and C_L/C_D yielding a $\gamma \simeq -3$ deg), the pitching-moment coefficient is extremely nose-down and would preclude the possibility of trimming the configuration at this condition. Thus, as with most powered lift systems, it is not C_L and C_D that present problems but obtaining pitch trim that remains the limiting factor in the usefulness of these concepts.

F-15 with Rotating Vane Thrust Reversers

MACAIR, NASA Langley, AFWAL, and Pratt and Whitney are involved in a joint research project to determine the effects of reverse thrust on the low-speed aerodynamics of fighter aircraft. There are problems associated with using reverse thrust on any aircraft; however, when the relatively high approach speeds for fighter aircraft are combined with the relatively short runways that the Air Force STOL requirements are projecting, a very significant problem area is identified—the engines must be at or near military power on approach. This requirement arises because the time it takes for an engine to spool up from near flight idle to military power is about the same time increment required for the entire short landing sequence.

One promising method of spoiling thrust on approach and providing full reverse thrust on landing is the rotating vane concept shown in Fig. 16. The rotating vanes can be deflected at an angle (nozzle vector angle) that permits the aircraft to maintain the thrust vector needed for approach while the engine is maintaining military power. The excess thrust is spoiled by symmetric deflections of the upper and lower vanes. Approach thrust can be varied by changing the nozzle vector angle rather than by variation in throttle setting. Once

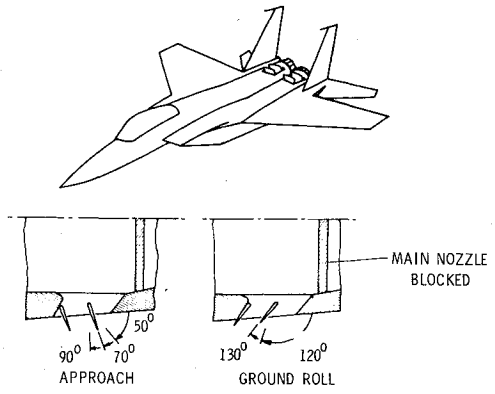

Fig. 16 Rotating vane thrust reverser concept.

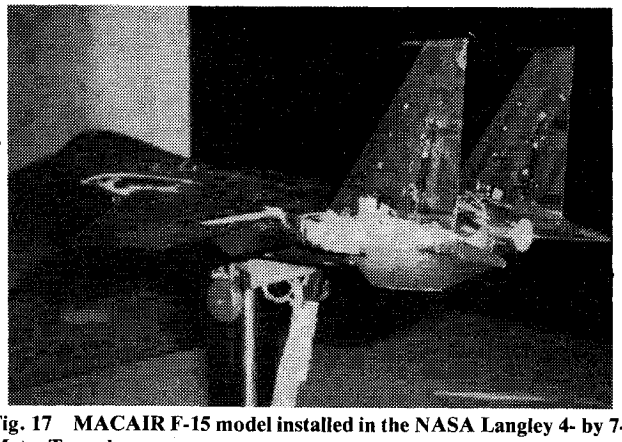

Fig. 17 MACAIR F-15 model installed in the NASA Langley 4- by 7-Meter Tunnel.

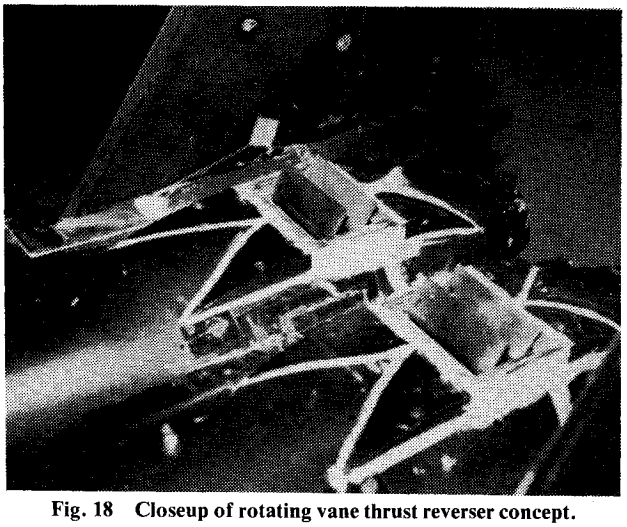

Fig. 18 Closeup of rotating vane thrust reverser concept.

the aircraft has made contact with the ground, the vanes can be quickly (on the order of 1 s) rotated forward to a full reverse vector angle of from about 120 to 130 deg, and military power reverse thrust is available shortly after touchdown. If this rotation were to be initiated, say, 1 s before touchdown, it may be possible to have full reverse thrust at wheel contact. Furthermore, if needed, the vanes can be deflected independently to provide a powerful pitch control capability to augment the horizontal tail.

An F-15 model has been tested in the NASA Langley 4- by 7-Meter Tunnel and an installation photograph is shown in Fig. 17. This model was equipped with a rotating vane thrust reverser (see Fig. 18). The longitudinal aerodynamic

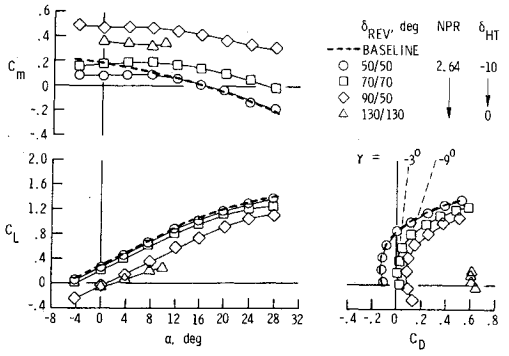

Fig. 19 Longitudinal aerodynamics of F-15 model with rotating vane thrust reversers at several vector angles.

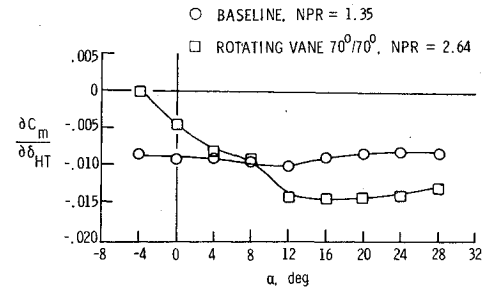

Fig. 20 Horizontal-tail power for F-15 model with and without partial thrust reversing.

characteristics of this installation are presented in Fig. 19. The data of Fig. 19 show that the military power settings (NPR = 2.64), the lift-curve slope relative to the baseline data is basically unchanged at nozzle vector angles from 50 to 70 deg, with a slight negative shift in $C_{L,0}$ at 70 deg/70 deg. At an unsymmetric vector angle of 90 deg/50 deg, there is, of course, a substantial negative shift in $C_{L,0}$; however, C_{L_α} is basically unaffected. The lift curve is reduced at the 130-deg nozzle vector angle for full reverse thrust in ground effect. The primary effect of nozzle vector angle on C_m appears to be increases in $C_{m,0}$ at increasing vector angles, especially for the 90 deg/50 deg which produces large nose-up moments. There are some changes in the slope of the pitching-moment curve (C_{m_α}) below $\alpha = 12$ deg. However, it is unclear whether or not this loss of stability is due to an installation problem (i.e., an interference between the large post mount and the horizontal tail) or is directly due to the exhaust plume. The drag polars are shifted by the vector component of thrust as the nozzle vector angle is increased. The 90 deg/50 deg configuration should produce about the same thrust as the 70 deg/70 deg, assuming each nozzle is passing equal mass flow. Since it produces considerably less thrust, it appears that more of the mass flow is exiting out the top vane at 90 deg than the bottom vane at 50 deg. The large C_D produced for the 130 deg/130 deg nozzle vector angle is equivalent to 53% of military thrust, which is consistent with target values of from approximately 50 to 60% of military thrust. It should be noted that the data for the 130 deg/130 deg nozzle were obtained in ground effect, whereas the previous examples of approach reverse thrust were obtained out-of-ground effect. From the flight-path lines on the figure, it appears that a nozzle vector angle of about 60 deg/60 deg will be required if a $\gamma = -4$-deg approach were to be flown. This would probably be a lower limit for approach angle, and the upper limit of -7 or -8 deg can be achieved with a nozzle vector angle of 70 deg/70 deg. Therefore results from the 70 deg/70 deg configuration will be used to show directional stability, rudder power, and horizontal tail power.

The horizontal tail power $\partial C_m / \partial \delta_{HT}$ shown in Fig. 20 for the baseline F-15 with flight idle (NPR = 1.35) thrust setting is

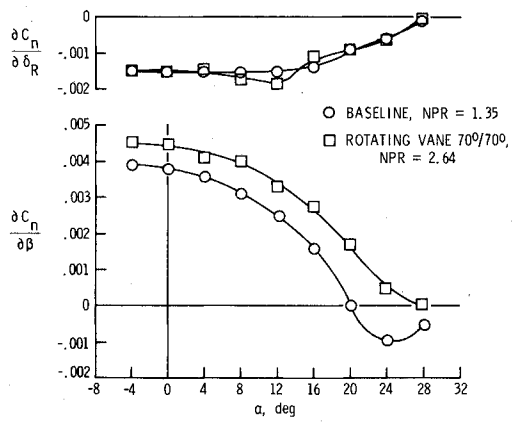

Fig. 21 Directional stability and rudder power for F-15 model with and without partial thrust reversing.

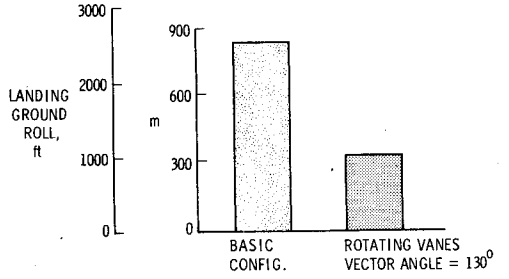

Fig. 22 Estimated minimum ground roll for F-15 with and without thrust reversing.

about constant with angle of attack. The values of $\partial C_m/\partial \delta_{HT}$ for the 70 deg/70 deg configuration at military power settings increase from 0 at -4-deg angle of attack to about a constant -0.014 above $\alpha = 12$ deg. This level is about 50% greater than the baseline. The reduction in $\partial C_m/\partial \delta_{HT}$ and loss of longitudinal stability mentioned previously at low angles of attack are usually attributed to a reduction in dynamic pressure at the tail due to the effect of the exhaust jet. However, as mentioned earlier, it is unclear as to whether or not this is an installation problem or a direct effect of the exhaust plume.

The rudder power and directional stability are presented in Fig. 21, and there is essentially no change in rudder power from the baseline F-15 to the 70 deg/70 deg configuration. There is a modest increase in directional stability throughout the angle-of-attack range for the 70 deg/70 deg configuration when compared to the baseline F-15. The reduction in C_{n_β} at high α for the baseline F-15 is also apparent in the 70 deg/70 deg data. Overall, it would appear that the 70 deg/70 deg nozzle vector angle at military power setting would be a viable configuration for in-flight thrust reversing for approach.

Once the airplane is on the ground, the 130-deg nozzle vector angle appears to offer the needed reverse thrust performance for reduced ground roll. A comparison of maximum performance (i.e., minimum distance) landing ground roll for a baseline F-15, and the 130 deg/130 deg nozzle vector angle is shown in Fig. 22. Assumptions for baseline ground roll were idle thrust and maximum wheel braking on dry runway at touchdown. The assumptions for the reverse thrust ground roll were reverse thrust and wheel braking available on wheel touchdown, dry runway, and reverse thrust available to zero velocity. With these assumptions, the maximum performance ground roll can be reduced from about 762 m (2500 ft) to 244 m (800 ft). Of course, dispersion, wet runways, and a delay in application of full reverse thrust or reverse thrust cutoff at velocities greater than zero will considerably increase the landing ground roll.

Concluding Remarks

NASA Langley Research Center has conducted wind tunnel investigations in the Langley 4- by 7-Meter Tunnel of a concept which uses spanwise blowing on a trailing-edge flap and a thrust reverser concept for an F-15 configuration.

Using spanwise blowing on the trailing-edge flap has indicated that a fairly significant lift increment is possible when an under-the-wing blowing cascade is used in conjunction with large flap deflections. Since a portion of the trailing edge was unaffected by the spanwise flow, it would appear that further increases in induced lift are possible if the spanwise flow can be distributed over the entire flap. This lift increment is, however, accompanied by the large nose-down pitching moments typical of vectored thrust concepts.

An investigation of the effects of reverse thrust on the low-speed aerodynamics of an F-15 configuration indicates that a rotating vane concept will provide the partial thrust required for approach while maintaining military power settings, and effective reverse thrust for a significant reduction in ground roll. It appears that in the angle-of-attack range required for approach, the F-15 with the rotating vane thrust reverser maintains adequate rudder and horizontal tail power as well as directional stability.

References

[1] Paulson, J.W. Jr. and Thomas, J.L., "Summary of Low-Speed Longitudinal Aerodynamics of Two Powered Close-Coupled Wing-Canard Fighter Configurations," NASA TP-1535, 1979.

[2] Paulson, J.W. Jr. and Thomas, J.L., "Effect of Twist and Camber on the Low-Speed Aerodynamic Characteristics of a Powered Close-Coupled Wing-Canard Configuration," NASA TM-78722, 1978.

[3] Paulson, J.W. Jr., Thomas, J.L., and Winston, M.M., "Transition Aerodynamics for Close-Coupled Wing-Canard Configuration," AIAA Paper 79-0336, Jan. 1979.

[4] Paulson, J.W. Jr., "An Analysis of Thrust-Induced Effects on the Longitudinal Aerodynamics of STOL Fighter Configurations," AIAA Paper 80-1879, Aug. 1980.

[5] Paulson, J.W. Jr., "Tactical Aircraft Research and Technology, Thrust Aerodynamics of STOL Fighter Configurations," NASA CP-2162, Tactical Aircraft Research and Technology, Part 2, Vol. 1, Oct. 1980.

[6] Whitten, P.D., "An Experimental Investigation of a Vectored-Engine-Over-Wing Powered-Lift Concept," U.S. Air Force Flight Dynamics Laboratory Technical Report AFFDL-TR-76-92, Vol. II-High Angle of Attack and STOL Tests, March 1978.

[7] Leavitt, L.D. and Yip, L.P., "Effects of Spanwise Nozzle Geometry and Location on the Longitudinal Aerodynamic Characteristics of a Vectored Engine-Over-Wing Configuration at Subsonic Speeds," NASA TP-1215, 1978.

[8] Whitten, P.D. and Howell, G.A., "Investigations of the VEO-Wing Concept in Air-To-Ground Role," U.S. Air Force Flight Dynamics Laboratory Technical Report AFFDL-TR-79-3031, March 1979.

[9] Stumpfl, S.C., "Vectored-Engine-Over-Wing Concept Development," *Proceedings V/STOL Aircraft Aerodynamics*, Vol. II. Naval Postgraduate School, Monterey, Calif., May 1979, p. 850.

[10] Paulson, J.W., Whitten, P.D., and Stumpfl, S.C., "Wind-Tunnel Investigation of the Powered Low-Speed Longitudinal Aerodynamics of the Vectored-Engine-Over (VEO) Wing Fighter Configuration," NASA TM 83263, March 1982.